THE JOURNAL OF PHYSICAL CHEMISTRY A

 VOLUME 107, NUMBER 16, APRIL 24, 2003

# ARTICLES

## Site Specific Solvation Statics and Dynamics of Coumarin Dyes in Hexane−Methanol Mixture

**Tatiana Molotsky and Dan Huppert***

*Raymond and Beverly Sackler Faculty of Exact Sciences, School of Chemistry, Tel Aviv University, Tel Aviv 69978, Israel*

*Received: October 25, 2002; In Final Form: January 28, 2003*

We have studied the solvation statics and dynamics of coumarin 153 and 102 dyes in hexane−methanol mixtures. The solvation of the coumarin dyes, both in the ground and in the excited electronic states, exhibits a nonlinear solvatochromic shift in the methanol mole fraction. The solvation dynamics of both dyes in their excited states are rather slow and depend on the mixture composition. The statics and dynamics of the spectroscopic data are attributed mainly to the formation of a hydrogen bond between methanol and the carbonyl group of the coumarin dye. IR spectra of the coumarin dyes in these binary mixtures confirm the formation of hydrogen bonding with the carbonyl group. We analyzed the statics and dynamics of the solvation of coumarin dyes in a hexane−methanol mixture using a model of two distinct solvates. The first solvate is a coumarin dye which is not hydrogen bonded at the carbonyl group. The second solvate has a specific hydrogen bond between the hydroxyl group of the methanol and the carbonyl group of the coumarin dye. The excited-state dynamics are followed by time-resolved emission, and the analysis is based on the irreversible diffusion-influenced chemical reaction formalism.

### Introduction

Solvation statics and dynamics have been extensively studied.[1−6] Ultrashort laser pulses of pico- and femtosecond time duration have been used during the last 2 decades to study solvation processes on a femto−picosecond time scale. In these studies, the solvation dynamics were monitored via the time-dependent spectral shift of the fluorescence band of a probe molecule dissolved in the solvent under study. Until recently, most studies of solvent dynamics were conducted in neat polar solvents, while only a few studies of solvation dynamics in mixtures of nonpolar and polar solvents exist.[7−19]

Another class of binary solvent solutions is the mixture of two polar solvents with approximately the same polarity. Barbara and co-workers[20] and, recently, Maroncelli and co-workers[21] studied the solvation dynamic characteristics of a probe molecule in two polar liquid mixtures. The neat liquids are both aprotic solvents, the equilibrium solvation properties of which are sufficiently similar that the occurrence of preferential solvation is not expected in their binary mixtures. Gardecki and Maroncelli[21] found that the steady-state solvent nuclear reorganization energy in these mixtures is essentially invariant to the composition of these mixtures. Solvation times of the binary mixtures vary, between the pure solvent limits, with the composition of solvent mixtures. The dependence of the characteristic solvation times on composition is related to other dynamic properties, such as solute rotation times and solution viscosity. Furthermore, the dependence of the dynamics on the composition can be described by a linear function of the mole fraction of one of the solvent mixture constituents.

Suppan[7] studied the effect of solvent mixtures of different dielectric polarities on the absorption and emission of polar

* Corresponding author. E-mail: huppert@tulip.tau.ac.il. Fax/telephone: 972-3-6407012.

10.1021/jp022317m CCC: $25.00 
Published on Web 04/02/2003

solute probes. In such solvent mixtures, a process of preferential solvation, described as "dielectric enrichment", occurs in the solvation shell of dipolar solute molecules. The solute−solvent interaction energy is a linear function of the solvent polarity. The polarity of a solvent is defined as a function, $F$, of the dielectric constant, $\epsilon$. Onsager's function is given by

$$F = \frac{2(\epsilon - 1)}{2\epsilon + 1} \tag{1}$$

The polarity of an "ideal" mixture of two solvents, composed of nonpolar, N, and polar, P, solvents, whose dielectric constants are $\epsilon_N$ and $\epsilon_P$ respectively is a simple linear combination according to their mole fractions $x_N$ and $x_P$

$$F_{\text{linear,bulk}} = x_N F_N + x_P F_P \tag{2}$$

Dielectric "nonideality" of a binary solvent system refers to the deviation of the Onsager reaction field function from linearity in the polar mole fraction of the solvent mixture. A dipolar fluorophore, dissolved in an ideal dielectric mixture, exhibits a solvatochromic shift that is linear in the solvent polar mole fraction in its solvation sphere. As a result, the "local composition" can easily be determined from the peak shift. Kauffman and co workers[8,9] have identified conditions under which the linear approximation is justified, and find that, for most cases of practical importance, the linear approximation will not provide accurate estimates of the local solvent composition from solvatochromic studies. Similarly, solvatochromic shifts can only be accurately predicted from theoretical local compositions if dielectric nonideality is taken into account.

In a previous study,[22] we measured the solvation energetics and dynamics of coumarin 153 in a solvent mixture of hexane−propionitrile. The solvation of coumarin 153 in this mixture shows that distinct preferential solvation occurs both in the ground and excited states. Recently, Agmon[23] applied the theory of a reversible diffusion-influenced reaction to the solvation statics and dynamics of a probe molecule in binary mixtures. The theory involves many aggregates of a solute surrounded by several polar solvent molecules in the first solvation shell, such as $PS_N^{n-i}S_P^i$, where $i \geq 1$. $PS_N^n$ denotes $n$ nonpolar solvent molecules and $PS_N^{n-i}S_P^i$ denotes $i$ polar molecules in the first solvation shell. We successfully used Agmon's model for preferential solvation to explain both the static and dynamic spectroscopic results of a coumarin hexane−propionitrile solution.

Rempel and co workers[16] measured a time-resolved Stokes shift and the steady-state absorption and fluorescence of coumarin 153 in binary mixtures of alcohols and alkanes at various alcohol concentrations. Depending on the alcohol concentration, the Stokes shift occurs on a time scale ranging from 300 ps to several nanoseconds. They explained their results along the lines of Suppan's theory[7] of preferential solvation with nonspecific interaction.

Recently Jarzeba and co-workers[24] studied the solvation statics of coumarin 153 in toluene−methanol mixtures. For the excited coumarin 153 in toluene−methanol mixtures, strong nonlinearity in the fluorescence solvatochromic shifts is attributed mainly to formation of a hydrogen bond between methanol and coumarin 153. IR spectra of coumarin 153, in solvent mixtures containing methanol, confirm the formation of a hydrogen bond between methanol and coumarin 153.

Previously Solntsev, Huppert, and Agmon[25,26] studied steady state and time-resolved fluorescence of 5-cyano-2-naphthol (5CN2OH) in various neat solvents. The extremely high photoacidity of cyanonaphthols results in large solvatochromic shifts. The solvatochromism of 5CN2OH demonstrated the dominant role of specific solvation. Stabilization by a single hydrogen bond, between the photolabile hydroxylic hydrogen and proton-accepting solvents, has a magnitude similar to that of nonspecific polar solvation.

The case of a specific interaction of a solvent molecule at a certain site of a probe molecule is a special case that needs to be treated by a different model than the dielectric enrichment model. In this study, we measure the solvation energetics and dynamics of coumarin 153 and 102 in hexane−methanol mixtures. The main findings of our study are that the red shift of the emission band of both coumarin dyes in these mixtures is much larger than that of hexane−propionitrile mixtures. In contrast, the red shift of the absorption band of the coumarin dyes in hexane−methanol mixtures is smaller than that in hexane−propionitrile mixtures. The Onsager dielectric function of hexane−methanol mixtures shows that the emission band shift cannot solely arise from dielectric enrichment, but another mechanism contributes a large fraction of the spectral shift. The bathochromic spectral shift, as a function of methanol concentration in the mixture, is mainly attributed to the formation of a hydrogen bond between methanol and the carbonyl group of the coumarin dye. To account for the specific binding of a methanol molecule we used a model of two distinct solvates to describe the experimental results via the hydrogen-bonding reaction $P + S \rightarrow PS^H$ where P denotes a probe molecule in which the carbonyl group is not hydrogen bonded. $PS^H$ is the probe molecule hydrogen bonded at the carbonyl group with a methanol molecule and S denotes a non-hydrogen bonded methanol molecule.

**Experimental Section and Line Shape Analysis**

Time-resolved fluorescence was detected using a time-correlated single-photon-counting (TCSPC) technique. As a sample excitation source, we used a CW mode-locked Nd:YAG-pumped dye laser (Coherent Nd:YAG Antares and a cavity dumped 702 dye laser) which provided a high repetition rate of short pulses (2 ps at full width at half-maximum (fwhm)). The TCSPC detection system is based on a multichannel plate Hamamatsu 3809 photomultiplier and a Tennelec 864 TAC and 454 discriminator. A personal computer was used as a multichannel analyzer and for data storage and processing. The overall instrumental response was about 40 ps (fwhm). Measurements were taken at 10 ns full scale. The samples were excited at 310 nm (the second harmonic of the Rhodamine 6G dye laser). At this wavelength, a sample is excited to $S_2$, the second excited electronic state. The transition dipole moment $S_0-S_2$ is perpendicular to $S_0-S_1$. Therefore, a polarizer, set at an angle complementary to the "magic angle", was placed in the fluorescence collection system.

Absorption spectra were acquired with a Perkin-Elmer model 551S UV−vis spectrometer. Steady-state fluorescence spectra of the samples were recorded on an SLM-Aminco-Bowman 2 luminescence spectrometer and corrected according to manufacturer specifications. IR spectra were recorded using an EQVINOX 55/S spectrometer.

Coumarin 153 and 102 (C153 and C102) were purchased from Exciton and were used without further purification. Hexane and methanol were purchased from Aldrich and used without further purification. Methanol has a limited miscibility in hexane, up to 0.1 mole fraction, $x_P$. Hexane−methanol mixtures were prepared at 0.013, 0.025, 0.05 and 0.1 mole fraction, $x_P$, of methanol. All experiments were performed at room temperature (23 ±2 °C).

**Spectral Analysis of Line Shapes.** The shape of the absorption of both coumarin dyes in hexane−methanol mixtures could not be fitted with a log-normal distribution since the vibronic structure in the absorption spectrum is preserved to about 0.1 mole fraction of methanol. To fit the absorption line shape, $A(\nu)$, of C102 and C153 for all mixtures from 0 to 0.1 mole fraction we used eq 3[27]

$$A(\nu) = \sum_{k=0}^{\infty} \frac{S_0^{\,k}}{k!} \exp\left\{-\mathrm{cc}\left[\left(\frac{\nu - \nu_p}{\nu_{st}}\right) - k\frac{\nu_0}{\nu_{st}}\right]^2\right\} \qquad (3)$$

where $\mathrm{cc} = h\nu_{st}/2k_BT$ is the curvature of the ground and excited-state parabola in the solvent coordinate, $S_0$ the vibronic displacement of the excited-state parabola, $\upsilon_{st}$ the Stokes shift and $\upsilon_0$ the vibronic frequency modulating the spectral shape. The peak position of the absorption band is defined as $\upsilon_p = \upsilon_{12} - \upsilon_{st}$. $\upsilon_{12}$ is the electronic origin of the transition in the gas phase.

In contrast to the structured line shape of the absorption band, the emission band of hexane−methanol mixtures is broad and structureless and can be described by a log-normal distribution function.[1,28,29]

$$I(\nu) = h\begin{cases}\exp[-\ln(2)\{\ln(1+\alpha)/\gamma\}^2] & \alpha > -1 \\ 0 & \alpha \le -1\end{cases} \qquad (4)$$

with

$$\alpha \equiv 2\gamma(\nu - \nu_p)/\Delta$$

where $I(\upsilon)$ is the fluorescence intensity at frequency ($\upsilon$), $h$ the peak height, $\nu_p$ the peak frequency, and $\gamma$ the asymmetry parameter and $\Delta$ represents the band's width.

## Results and Discussion

This section is divided into five subsections.

In the first subsection we analyze both the absorption and emission spectra of the coumarin dyes in neat solvents using the Kamlet−Taft solvation scale. We show that both C102 and C153 have strong acid base properties in addition to their well-known polar properties. The second subsection describes briefly the published results of experimental and molecular dynamics simulations of hydrogen bonding of protic solvents to coumarin dyes. Next we present our simple single site-specific hydrogen-bonding model. This model is similar to the model that we previously used successfully to describe the solvation of coumarin dyes by cations in electrolyte solutions.[29,30] We then describe and analyze the absorption, emission and IR spectra of the coumarin dyes in hexane−methanol mixtures. The last subsection is devoted to the time-resolved emission results and their analysis using the site-specific model.

**1. Analysis of the Absorption and Emission Spectra in Neat Liquids.** *Absorption Spectrum in Neat Liquids.* Many compounds exhibit solvatochromic spectral changes, both in their absorption spectrum as well as in their fluorescence and/or phosphorescence spectra. The Kamlet−Taft[31,32] solvatochromic scale uses several parameters to describe and quantify the various contributions. The $\pi^*$ scale is an index of solvent dipolarity/polarizability, which measures the ability of the solvent to stabilize a charge or dipole by virtue of its dielectric effect. The $\alpha$ scale of solvent hydrogen bond donor (HBD) acidities describes the ability of the solvent to donate a proton in a solvent-to-solute hydrogen bond. The $\beta$ scale of hydrogen bond acceptor (HBA) basicities provides a measure of the solvent's ability to accept a proton (donate an electron pair) in a solute-to-solvent hydrogen bond.

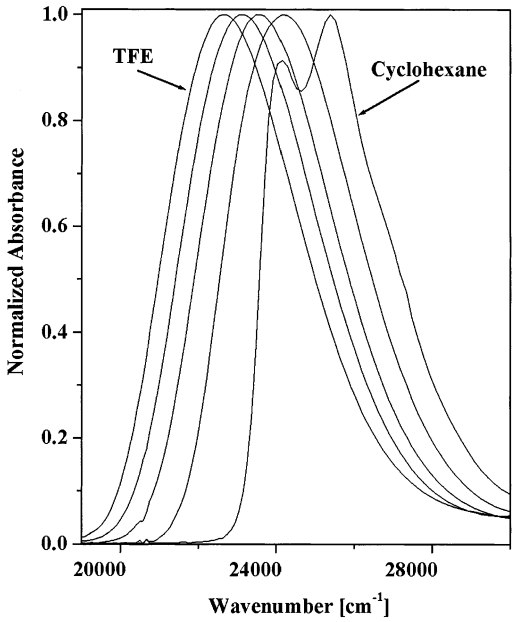


**Figure 1.** Absorption spectra of coumarin 153 in various solvents with different $\pi^*$, $\beta$, and $\alpha$ properties. Left to right: trifluorethanol (TFE), dimethylformamide (DMFA), ethanol (EtOH), ethyl acetate (EtOAc), and cyclohexane.

Figure 1 shows the absorption spectra of C153 in various solvents with different $\pi^*$, $\beta$, and $\alpha$ properties. We fitted the experimental spectra using a log-normal function (fit not shown). The absorption band peak positions, as well as all the solvents' $\pi^*$, $\beta$, and $\alpha$ parameters, are displayed in Table 1. As the solvent polarity, $\pi^*$, increases, the band position shifts to the red. The linear regression fit of 12 solvents to eq 5

$$\nu = \nu_0 + p\pi^* + a\alpha + b\beta \qquad (5)$$

yielded $\nu_0 = 24.90 \times 10^3$ cm$^{-1}$, $p = -1780$ cm$^{-1}$, $a = -540$ cm$^{-1}$, and $b = 150$ cm$^{-1}$ with $R$, the correlation coefficient, being 0.94.

Using Maroncelli's[33] data on the C102 absorption position in 6 solvents, the solvent parameters of which are given in Table 1, yielded $\nu_0 = 28.30 \times 10^3$ cm$^{-1}$, $p = -2230$ cm$^{-1}$, $a = -1210$ cm$^{-1}$, and $b = 500$ cm$^{-1}$ with $R = 0.98$. The two coumarins differ only slightly in their chemical structure—the $CH_3$ group at position 4 in C102 is replaced by a $CF_3$ group in C153. This small structural change red shifts the $\nu_0$ of C153 by $\sim$3500 cm$^{-1}$ and decreases both its polarity and HB properties.

*Emission Spectrum in Neat Liquids.* The emission spectra of C153 in various solvents are shown in Figure 2. In general, the band shifts to the red with solvent polarity. In hexane, as expected from the absorption spectrum (nonpolar solvent), a vibronic structure is also superimposed on the emission. In contrast to the absorption band, the emission bandwidth shrinks considerably in more polar liquids. Also, we find a large bathochromic shift with HBD solvents, while HBA solvents shift the emission spectrum to the blue. The vibrational substructure seen in apolar liquids disappears in polar and HB liquids.

A linear regression fit of the emission band position of C153 in neat solvents to the Kamlet−Taft scale with the solvent parameters $\pi^*$, $\alpha$, and $\beta$

$$\nu^* = \nu_0^* + p^*\pi^* + a^*\alpha + b^*\beta \qquad (6)$$

**TABLE 1: Peak Absorption and Emission Frequencies of C102 and C153 in Different Solvents, with Their Corresponding Kamlet−Taft Parameters**

| | Kamlet−Taft parameters | | | C153 | | C102 | |
|---|---|---|---|---|---|---|---|
| solvent[a] | $\pi^{*}$ [b] | $\beta$[c] | $\alpha$[c] | $\nu_p$(abs) $\times 10^3$ ($cm^{-1}$)[d] | $\nu_p$(em) $\times 10^3$ ($cm^{-1}$)[e] | $\nu_p$(abs) $\times 10^3$ ($cm^{-1}$)[f] | $\nu_p$(em) $\times 10^3$ ($cm^{-1}$)[f] |
| DMSO | 1 | 0.76 | 0 | 23.30 | 19.00 | 26.50 | 21.20 |
| DMFA | 0.88 | 0.69 | 0 | 23.10 | 18.90 | 26.70 | 21.50 |
| TFE | 0.73 | 0 | 1.51 | 22.70 | 18.70 | 24.65 | 20.60 |
| ACN | 0.66 | 0.31 | 0.19 | 23.75 | 19.35 | 26.80 | 21.50 |
| MeOH | 0.6 | 0.62 | 0.93 | 23.50 | 18.85 | 26.20 | 20.50 |
| THF | 0.55 | 0.55 | 0 | 24.10 | 20.10 | 27.45 | 22.55 |
| EtOH | 0.54 | 0.77 | 0.83 | 23.60 | 19.05 | | |
| 1,4-dioxane | 0.49 | 0.37 | 0 | 24.25 | 20.45 | | |
| EtOAc | 0.45 | 0.45 | 0 | 24.15 | 20.10 | | |
| Et2O | 0.24 | 0.47 | 0 | 24.45 | 21.35 | | |

[a] Acronyms: acetonitrile (ACN), ethanol (EtOH), methanol (MeOH), dimethyl sulfoxide (DMSO), trifluoroethanol (TFE), dimethylformamide (DMFA), ethyl acetate (EtOAc), tetrahydrofuran (THF), and diethyl ether (Et2O). [b] From ref 32. [c] From ref 31. [d] Frequency of the absorption maximum in $cm^{-1}$, as obtained from a fit to the log-normal distribution. [e] Peak frequency of the emission spectrum, in $cm^{-1}$. [f] From ref 33.

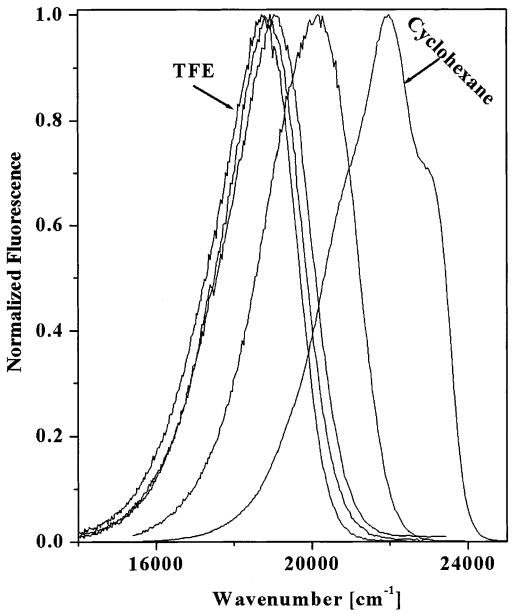


**Figure 2.** Emission spectra of C153 in various solvents. Left to right: TFE; DMFA; EtOH; EtOAc; cyclohexane.

yielded $\nu_0^* = 21.83 \times 10^3$ $cm^{-1}$, $p^* = -2620$ $cm^{-1}$, $a^* = -860$ $cm^{-1}$, and $b^* = -680$ $cm^{-1}$ with $R = 0.9$. Using Maroncelli's[33] data for the emission band position of C102, we find $\nu_0^* = 23.58 \times 10^3$ $cm^{-1}$, $p^* = -3200$ $cm^{-1}$, $a^* = -1980$ $cm^{-1}$, and $b^* = 1060$ $cm^{-1}$ with $R = 0.97$.

The analysis of the absorption properties and their excited-state emission spectra of both dyes, show that $\nu_0$ and $\nu_0^*$ differ substantially; the ground state, $p$, value for C102 is larger than that of C153. Both compounds have mild HB properties in the ground state while, in the excited state, both compounds have a larger dipole moment, $\mu_e > \mu_g$, and much larger HB properties, especially the $a$ parameter (tendency to accept a hydrogen bond from a hydrogen bond donating solvent). For C102 in methanol ($\alpha = 0.93$), the red spectral shift, due to hydrogen bond formation, is about the same as that of the dipole moment interaction. Using eq 6, one can calculate the three contributions to the total fluorescence red shift of C102 in methanol with respect to hexane. The red shift, due to the dipole moment, is 1920 $cm^{-1}$, about the same as that due to the hydrogen bonding of the carbonyl group of the coumarin with the hydroxyl group of the methanol, i.e., 1840 $cm^{-1}$. The $b$ parameter shows the tendency of the probe molecule to donate a hydrogen bond to a hydrogen bond accepting solvent. The tendency of C102 to donate a hydrogen bond is larger in the ground state and hence causes a blue-shift rather than a red shift. The $\beta$ parameter of methanol is 0.62, smaller than $\alpha = 0.93$. The $b\beta$ term in eq 6 for C102 in neat methanol contributes a blue shift to the emission band of about 600 $cm^{-1}$ compared with a red shift of 1840 $cm^{-1}$ due to the HBA properties of the probe molecule.

**2. Hydrogen Bonding of Coumarin Dyes in Hydrogen-Bonding Solvents.** There are several reports concerning hydrogen bonding and the breaking of hydrogen bonds of coumarin dyes in protic solvents like alcohols or from other known hydrogen bond donors.

Time-resolved fluorescence spectra of three amino-substituted coumarin dyes have been recorded in methanol and dimethyl sulfoxide using the fluorescence upconversion technique by Gustavsson et al.[34] The three fluorinated coumarins are coumarin 151, coumarin 35, and coumarin 153. The dynamic Stokes shifts are found to be dominated by an ultrafast component with a characteristic time shorter than the time resolution of ≈50 fs. The dynamic Stokes shifts are compared with estimations based on a "Kamlet and Taft" analysis of steady-state data in 20 solvents. They found that the ultrafast component can be assigned mainly to intramolecular relaxation. The breaking of hydrogen bonds at the amino group is very fast in both solvents and embedded in the ultrafast solvent inertial relaxation, while the reformation of hydrogen bonds at the carbonyl group is believed to occur on the 10−20 ps time scale in the hydrogen bond donating methanol solvent. However, they concluded that it is impossible to unambiguously correlate a particular experimental time constant with the breaking or formation of a hydrogen bond.

The rotation times of C102 in Decalin and pure trifluoroethanol (TFE, a strongly hydrogen bond-donating solvent) and of the 1:1 complex of C102 and TFE in Decalin have been measured using time-resolved fluorescence methods by Maroncelli and co-workers.[35] The rotation of C102 in Decalin and C102:TFE complex in Decalin is described by the Debye−Stokes−Einstein equation, assuming slip hydrodynamics. The reduced rotation time, $\tau_r/\eta$, of C102 in neat TFE differs from its value in neat Decalin but is indistinguishable from that of the C102:TFE complex in Decalin. This observation suggests that the rotation of C102 in neat TFE can be interpreted in terms of the rotation via slip hydrodynamics of a 1:l complex. Thus, in TFE with the Kamlet−Taft hydrogen bond-donating power of the solvent, $\alpha = 1.51$, solvent attachment quantitatively explains the observed rotational dynamics.

Jarzeba and co-workers[24] studied the solvation statics of coumarin 153 in toluene−methanol mixtures. For the excited coumarin 153 in toluene−methanol mixtures, strong nonlinearity

in the fluorescence solvatochromic shifts is attributed mainly to formation of a hydrogen bond between methanol and coumarin 153. IR spectra of coumarin 153, in solvent mixtures containing methanol, confirm the formation of a hydrogen bond between methanol and coumarin 153.

Nibbering et al.[36] studied the hydrogen-bonding dynamics in the electronically excited state of C102 where they deduced that a hydrogen bond cleavage occurs within 200 fs. They compare the electronic absorption and emission properties of C102 hydrogen bonded to CHCl3, phenol or 2,2-dimethyl-3-ethyl-3-pentanol. They concluded that hydrogen bonding is coupled to the electronic transition and that the hydrogen bond cleavage is responsible for the electronic state change.

Ladanyi and Skaf,[37] using molecular dynamics simulations, studied the solvation dynamics following charge-transfer electronic excitation of diatomic solutes immersed in methanol−water mixtures. They found significantly different responses for the two solutes and related them to the fact that the solute with the smaller site diameters is a much better hydrogen bond acceptor than the larger diameter solute. For the small diameter solute in methanol and mixed solvents, they also calculated H-bond response functions, which measure the rate of solute−solvent hydrogen bond formation after the solute's excitation, and found that, for short times, the hydrogen bond formation is slower than the solvation dynamics while, for longer times, the solvation and hydrogen bond formation response functions decay at similar rates.

These reports[34−37] and the Kamlet−Taft analysis indicate that site-specific hydrogen bonding of protic solvents to coumarin dyes occurs both in the ground and excited states. From the Kamlet−Taft analysis of the fluorescence of the coumarin dyes in the excited-state we find stronger hydrogen bond accepting power than in the ground state. On the basis of the IR measurement, Nibbering et al.[36] concluded that the hydrogen bond, on the carbonyl group of a complex of coumarin with phenol, breaks upon electronic excitation within 200 fs. This result somehow conflicts with the picture that arises from other studies. It may be explained by the formation of hydrogen bonds at other sites on the electronically excited coumarin molecule. Gustavsson et al.[34] attributed 20 ps to the time of reformation of the hydrogen bond of the excited coumarin. Since the shortest time resolution in our experiments is limited to about 20 ps we cannot observe such short processes. The data analysis of our experiments on the long time domain of 20 ps to 5 ns will be based on our model site-specific hydrogen bonding of a single solvent molecule to a coumarin molecule.

**3. Model for Hydrogen Bonding.** In the rest of this paper, we report the results of the solvation statics and dynamics of the two coumarin dyes in hexane−methanol mixtures. The main finding concerns the large contribution to the solvation energy of the hydrogen bond between methanol and the coumarin dye.

The absorption spectrum, steady state emission, and time-resolved emission of C102 and C153 in hexane−methanol binary mixtures are strongly affected by the hydrogen bonding of a methanol molecule to the carbonyl of the coumarin. A topic related to site specific solvation is the effect of an electrolyte on the solvation of probe molecules. Previously, we studied the solvation energetics and dynamics of coumarin 153 in various electrolyte solutions of polar organic solvents.[29,30] We used a model of two distinct solvates to explain the experimental data. The first distinct solvate was a coumarin dye molecule surrounded by $n$ solvent molecules in the first solvation shell, $PS_n$. In the second distinct solvate, one of the surrounding solvent molecules in the first solvation shell was replaced by a cation, $PS_{n-1}I$. Upon photoexcitation of the coumarin dye, an ion−solvent exchange reaction occurred, followed by time-resolved fluorescence measurements. The model was successfully applied to coumarin 153 dye in all the solvents used, as well as a wide range of electrolyte concentrations. Maroncelli and co workers[33] used an extended model, which also included aggregates with several ions in the first solvation shell around the solute.

**SCHEME 1**

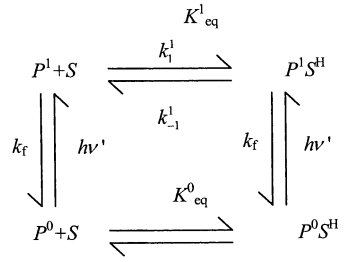


The hydrogen bonding by a methanol molecule to the coumarin dye can be described by Scheme 1.

The two solvates, $P^0$ and $P^0S^H$, the non-hydrogen-bonded and the hydrogen-bonded coumarin, respectively, are in equilibrium in the ground state. From the absorption spectra analysis we find an equilibrium constant of about, $K^0_{eq} \approx 2$. Therefore, in the ground state with a small concentration ($C < 0.6$ M) of the polar solvent, the major species in the solution is the non-hydrogen bonded coumarin. When a photon is absorbed by the solvate, $P^0$, to create $P^1$, a sudden increase in the basisity of the carbonyl group, as well as a large increase in the dipole moment (of about 8 D), occurs. It causes an increase in the equilibrium constant $K^1_{eq} > K^0_{eq}$ for hydrogen bonding (see Scheme 1). As a consequence, a hydrogen-bonding reaction occurs at the carbonyl group of the coumarin dye. The reaction rate constant is $>10^9$ s$^{-1}$, and hence a reaction is taking place within the excited-state lifetime, $\tau_f \approx 5$ ns. The overall hydrogen-bonding reaction rate depends on the methanol concentration and both the diffusion constant and the intrinsic reaction rate constant.

The absorption spectra of C102, at high methanol concentrations $\geq 0.2$ M, could not be fitted by the two-solvate model alone. In addition to the solvation, due to the specific hydrogen-bonding, one also needs to include a nonspecific dielectric enrichment contribution to the solvation energy to account for the total experimental red shift of both absorption and emission spectra. To account for the additional red shift, we extended the distinct solvate model and incorporated a nonspecific contribution to the solvation energy of the coumarin by dielectric enrichment in the framework of Suppan's model.[7] The emission spectra of both coumarin dyes could be fitted using the contributions of the specific hydrogen bonding and the nonspecific dielectric enrichment.

**4. Absorption, Emission, and IR Spectra in Hexane−Methanol Mixtures.** The absorption spectra of C102 and C153 in hexane−methanol mixtures are shown in Figure 3, parts a and b, respectively. The position, shape, and width of the absorption band depend on the solute−solvent interaction. We use the Kamlet−Taft[31,32] solvatochromic scale to quantify the spectral shifts. For comparison, we added to Figure 3, parts a and b, the absorption spectra of both coumarin in neat hexane ($\pi^* = 0$, $\alpha = \beta = 0$) and methanol ($\pi^* = 0.6$, $\alpha = 0.93$, $\beta = 0.62$). Unlike the spectrum in polar liquids, in hexane the spectrum also exhibits a vibrational substructure consisting of two peaks and a shoulder with $\sim$1300 cm$^{-1}$ spacing. For both dyes, when methanol is added, the absorption spectrum location is about the same as that in neat hexane. Comparing the

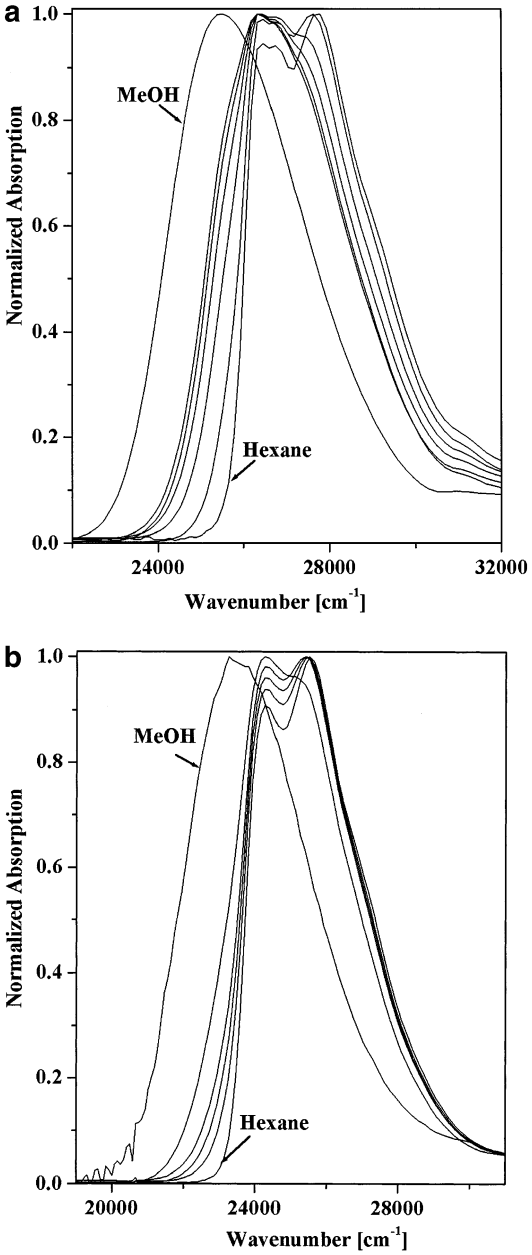


**Figure 3.** (a) Normalized absorption spectra of coumarin 102 in hexane−methanol mixtures with methanol mole fraction right to left: $x_P = 0$, 0.013, 0.025, 0.05, 0.08, 0.1, and 1. (b) Normalized absorption spectra of coumarin 153 in hexane−methanol mixtures with methanol mole fraction right to left: $x_P = 0$, 0.013, 0.025, 0.05, 0.1, and 1.

absorption band of both dyes in hexane−methanol mixtures, one finds a small difference at the red edge. A closer examination of the absorption spectra as a function of methanol concentration shows a consistent difference in the spectra of both dyes when methanol is added to hexane. Similar absorption changes are seen in studies of probe molecules in AOT−hexane−methanol reverse micelles.[38−40] The spectra of hexane−methanol mixtures can be fitted as a superposition of two bands. A blue band, which has characteristics similar to those of hexane, and a second band, the positions of which are ∼700 and ∼800 $cm^{-1}$ for C153 and C102 respectively, red-shifted with respect to the first. To fit the experimental data, we used eq 3 to generate the red band shape and also the band shape of the blue band which is similar to that of coumarin in hexane. The relative intensity of the red-shifted band increases with methanol. For both dyes, the red band intensity at about 0.1 mole fraction (about 1 M) of methanol is about that of the blue

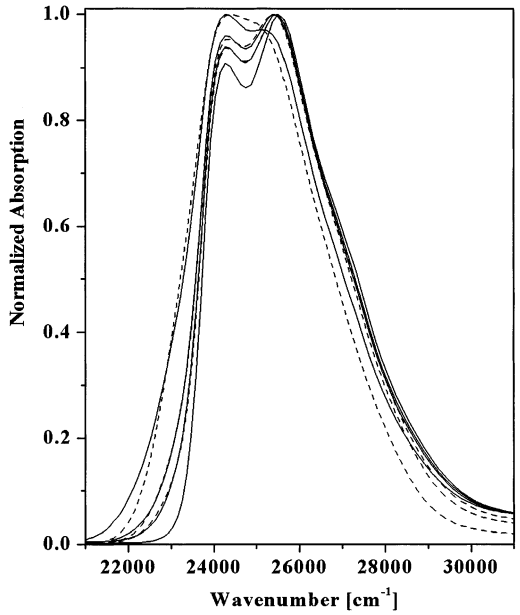


**Figure 4.** Normalized absorption spectra of coumarin 153 in hexane−methanol mixtures with methanol mole fraction right to left: $x_P = 0$; 0.013; 0.025, and 0.1. Solid lines are the experimental data, and dashed lines are the calculated fit.

**TABLE 2: Characteristic Parameters for a Two-Band Fit of the Absorption Bands of C153 and C102 in Hexane−Methanol Mixtures**

| | C153 | | C102 | | |
|---|---|---|---|---|---|
| $C$ (M) | $h_0$[a] | $\Delta\nu_{abs}$ ($cm^{-1}$)[b] | $h_0$[a] | $\Delta\nu_{abs}$ ($cm^{-1}$)[b] | $d$ ($cm^{-1}$)[c] |
| 0.1 | 0.84 | 590 | 0.83 | 700 | 0 |
| 0.2 | 0.72 | 590 | 0.70 | 800 | 150 |
| 0.4 | 0.57 | 590 | 0.54 | 800 | 200 |
| 0.83 | 0.39 | 690 | 0.36 | 800 | 250 |

[a] $h_0$ is the relative height of the non-hydrogen bonded species, $P$ peak maximum. [b] $\Delta\nu_{abs}$ is the band shift of the absorption band of the species $PS^H$ relative to $P$ in $cm^{-1}$ units. [c] $d$ is the nonspecific spectral shift, which shift both bands to the red.

band. Figure 4 shows the absorption spectra of C153 in hexane−methanol mixtures. The solid lines are the experimental data and the dashed lines show the computer-synthesized spectra. As the polar component increases, the vibronic structure is less pronounced. The vibronic structure disappears when $\upsilon_{st} \sim 2\upsilon_0$. In our case, we took five vibrations, $k = 4$, and $S_0 = 1.15$. For both C153 and C102 in neat hexane $\upsilon_{st} = 1700$ $cm^{-1}$ and $\upsilon_0 = 1350$ $cm^{-1}$. For the absorption spectra of C153 and C102 in neat methanol, $\upsilon_{st} = 3500$ and 3400 $cm^{-1}$, respectively. From the fit of the absorption spectrum of C153 and C102 in neat hexane, we find that $\upsilon_{12} = 26\,000$ and 28 200 $cm^{-1}$, respectively. For C153 and C102 in hexane−methanol mixtures, $\upsilon_{st} = 2290$ and 2500 $cm^{-1}$, respectively.

The relative intensities of the blue bands of both dyes, along with other relevant parameters, are given in Table 2. From the spectral analysis, the relative intensity of the red band (the HB band) of C153 is smaller than that of C102. The red band position is almost insensitive to the methanol concentration (methanol). For C102, it is about a half of the spectral shift between hexaneand neat methanol while, for C153, it is only a third of it. Even at the highest methanol concentration ($x_p = 0.1$), the double peak vibrational substructure is seen. The absorption spectrum depicts the relaxed solvent configuration around the ground state solute, where the time for the system to equilibrate is long. On the basis of the IR spectra and the absorption band position, shape, and width, we conclude that a

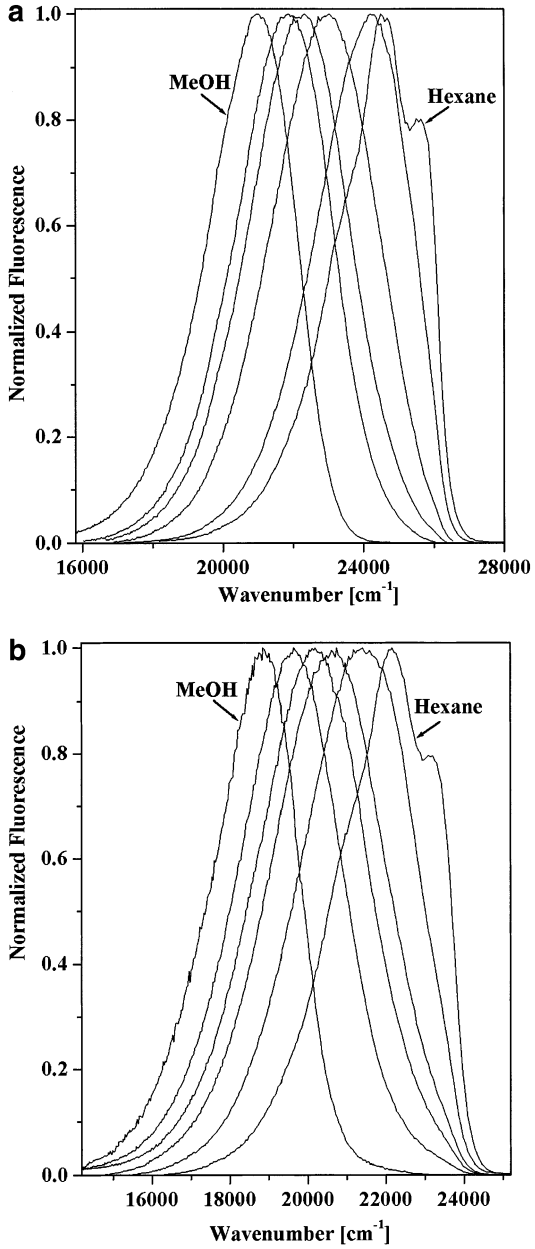


**Figure 5.** (a) Fluorescence spectra of coumarin 102 in hexane−methanol mixtures with methanol mole fraction right to left: $x_P = 0$, 0.013, 0.025, 0.05, 0.1, and 1. Excitation wavelengths are at the absorption maximum. (b) Fluorescence spectra of coumarin 153 in hexane−methanol mixtures with methanol mole fraction right to left: $x_P = 0$, 0.013, 0.025, 0.05, 0.1, and 1. Excitation wavelengths are at the absorption maximum

relatively large fraction of the dye molecules is hydrogen-bonded to a methanol molecule, even at a relatively low methanol mole fraction. We calculated the equilibrium constant, $K^0_{eq}$ (see Scheme 1), of the hydrogen-bonding reaction in the ground state. For C102 and C153, we found $K^0_{eq} = 2.1$ and 1.9, respectively.

*Emission Spectrum.* Parts a and b of Figure 5 show the emission spectra excited at the absorption band maximum of C102 and C153, respectively, in a hexane−methanol mixture. The band position and shape depend strongly on the methanol concentration. The larger the methanol concentration, the larger the red shift and the smaller the bandwidth. In both dyes, the emission band characteristics are similar.

While the absorption band position and shape of both coumarin dyes in the mixtures at all methanol concentrations are similar to those of the nonpolar solvent (hexane), the emission spectral behavior depends strongly on the methanol concentration. At 0.83 M, we find a large red band shift with respect to neat hexane; in C102, it is about 2850 $cm^{-1}$. In neat liquids, the band shift from hexane to methanol is ∼3680 $cm^{-1}$.

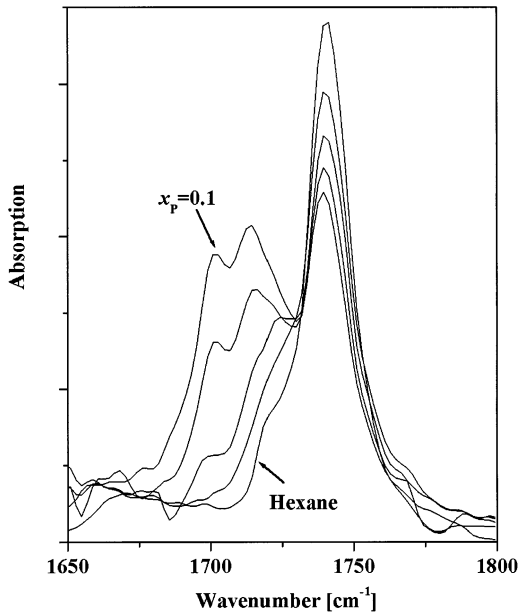


**Figure 6.** IR spectrum of the carbonyl stretching mode of C102 in hexane−methanol mixtures for methanol mole fraction $x_P = 0.013$, 0.025, 0.05, 0.08, and 0.1.

*IR Spectra.* Nibbering et al.[36] studied the formation of hydrogen bonds between C102 and phenol using femtosecond IR spectroscopy. They deduced that a hydrogen cleavage occurs within 200 fs. Recently, Jarzeba and co-workers[24] used IR absorption to study hydrogen bonding of the carbonyl group of C153 to methanol in toluene−methanol mixtures.

Figure 6 shows the IR spectrum of the carbonyl-stretching mode of C102 in hexane−methanol mixtures. In neat hexane, the absorption band is centered at ∼1740 $cm^{-1}$, and its intensity decreases with increasing concentration of the polar component in the mixture. Subsequently, a new red-shifted band appears which is centered at ∼1710 $cm^{-1}$ in neat methanol. An isosbestic point can be seen near 1731 $cm^{-1}$, showing the presence of equilibrium in the ground state between the hydrogen-bonded and non-hydrogen-bonded forms. Our IR absorption results are similar to those of Jarzeba and co-workers.[24]

*The Contribution of the Specific Hydrogen Bonding to the Spectral Red Shift.* Figure 7 shows the absorption and the emission peaks of coumarin 153 in both hexane−methanol and hexane−propionitrile mixtures[22] as a function of the polar component mole fraction, $x_P$. The absorption peak red shift of both coumarins 153 and 102 as a function of $x_P$ is smaller in hexane−methanol mixtures than in the corresponding mixture composition of hexane−propionitrile. In contrast to the absorption dependence on $x_P$, for the emission red shift, of both coumarin dyes, the dependence on $x_P$ is reversed. The emission band shift in hexane−methanol is appreciably larger than in the corresponding hexane−propionitrile mixtures. Figure 8 shows the dependence of the Onsager function, $F(\epsilon)$, as a function of $x_P$ for hexane−propionitrile[7] and hexanes−ethanol mixtures.[41]

Liquids are characterized by short-range order and long-range disorder. The correlation between the orientations (and also between the positions) due to the short-range ordering will lead to values of a multimer dipole, $M_i$, differing from $\mu$, the single molecule dipole. For this reason, Kirkwood[42] introduced a

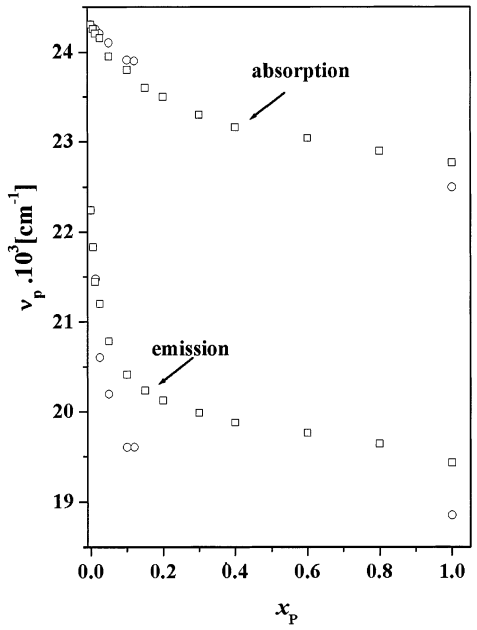


**Figure 7.** Peak of the absorption and emission spectra of coumarin 153 in a binary solvent mixture as a function of polar solvent mole fraction: methanol (open circles); propionitrile (open squares).

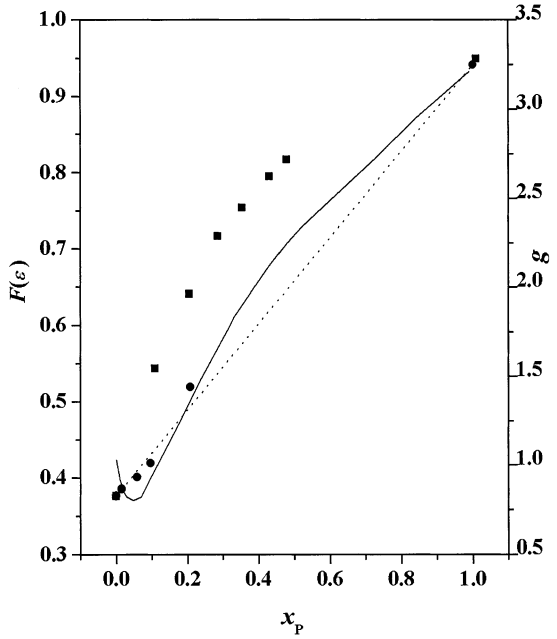


**Figure 8.** Polarity function $F(\epsilon)$ plotted as a function of the mole fraction of the polar solvent: hexane−propionitrile[7] (squares), hexanes−ethanol[41] (circles), and ideal mixture of hexanes−ethanol (dotted line). The Kirkwood correlation parameter, $g$ of ethanol in cyclohexane[43] is shown as a solid line.

correlation factor, $g$, which accounted for the deviations of the dielectric properties of the liquid from the value of the gas-phase dipole moment. The $g$ value of neat monol liquids like ethanol and methanol is about 3.2 at room temperature. The large $g$ value indicates that the average multimer dipole moment is much larger than the dipole moment of a single molecule.

In a mixture of monols with nonpolar solvents, monols show a minimum in $g$, indicating that, for the lower concentrations, the multimers with a small dipole moment dominate, even when the multimers with high dipole moment dominate in the pure state of the alcohol. This implies that, in general, the multimers with a small dipole moment will contain fewer molecules with a large dipole moment.[43]

The Kirkwood correlation factor, $g$, for cyclohexanes−ethanol at 298 K, taken from ref 43 as a function of $x_P$, is shown in Figure 8. From Figure 8 we can see that $F(\epsilon)$ for hexane−propionitrile mixtures deviate from the ideal mixture behavior and is larger than expected (positive deviation). In this case, the spectral shift of the absorption and emission bands, even without dielectric enrichment, will be significantly larger than expected from ideal mixture behavior. The opposite case is the mixture of hexane−methanol in which, up to about $x_P = 0.12$ (the largest miscible methanol mole fraction), the $F(\epsilon)$ function is smaller than predicted from the ideal case. In such a case, we expect smaller spectral shifts than the ideal solution in the absence of dielectric enrichment. Figure 7 shows a larger red shift of the emission band of coumarin 153 in a hexane−methanol solution than in hexane−propionitrile. The dipole moment of propionitrile in the gas phase is large, 3.5 D, while that of methanol is only 1.7 D. The methanol gas-phase dipole moment is about the same as THF, a much less polar liquid, being $\pi^* = 0.49$ ($\epsilon = 8$) compared with methanol where $\pi^* = 0.73$ ($\epsilon = 32.4$). Thus, it is expected that if $g < 1$ for methanol in hexane−methanol mixtures, the actual contribution to the spectral shift due to the dielectric enrichment process in these mixtures will be significantly smaller than that of a hexane−propionitrile mixture, which is a good example for dielectric enrichment studies. One possible large contribution to the red spectral shift of coumarin in hexane−methanol mixtures is that of hydrogen bonding of the methanol hydroxyl group to a negative site on the coumarin dye, possibly the carbonyl group. From the Kamlet−Taft solvatochromic scale, the α parameter, the hydrogen bond donating power of methanol, is 0.93 and the corresponding coumarin 102 hydrogen bond accepting value, $a$, is large, $a \cong -2000$ cm$^{-1}$. The contribution of the hydrogen bond, $\alpha a$, of methanol with coumarin to the emission spectral shift is about 1900 cm$^{-1}$. The hydrogen-bonding contribution is about the same as the polarity contribution, i.e., $\pi^* = 0.73$ and $p = -3000$ cm$^{-1}$; $\pi^* p \cong 2000$ cm$^{-1}$.

**5. Excited-State Dynamics in Hexane−Methanol Mixtures.** When the binary solution is irradiated by a short laser pulse at frequency $\nu'$, which coincided with the absorption band of the coumarin dye, both solvates, $P^0$ and $P^0S^H$, are excited. The relative probability of a photon being absorbed by the hydrogen-bonded solvate, $P^0S^H$, is given by

$$a(\nu') = \frac{ag^0(\nu')}{(1-a)f^0(\nu') + ag^0(\nu')} \tag{7}$$

where $a$ is the fraction of the $P^0S^H$ species in the ground state. $f(\nu')$ and $g(\nu')$ are the line shape functions of the ground-state absorptions of $P^0$ and $P^0S^H$, respectively.

When a photon is absorbed by the solvate $P^0$ to create $P^1$, a sudden large increase in the basisity of the carbonyl group, as well as a large increase in the dipole moment (of about 8 D), occurs. It causes a large increase in the equilibrium constant $K^1 > K^0$ for hydrogen bonding (see Scheme 1). As a consequence, a hydrogen-bonding reaction takes place at the carbonyl group of the coumarin dye. The following scheme illustrates the dynamics immediately after excitation of the solvate P:

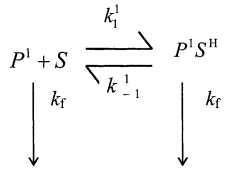

The zeroth-order description of the kinetics of the above scheme is based on the phenomenological rate equations of chemical kinetics. The mathematical solution of the appropriate coupled rate equations is given in ref 44. If $k_1^1 \gg k_{-1}^1$, $k_f$, then $P^1$ fluorescence intensity decays as a single exponential while exponential growth of the fluorescence intensity of $P^1S^H$ takes place. The decay rate of the $P^1$ species varies linearly with methanol concentration.

We used a diffusive model where the hydrogen bonding occurs at a certain rate whenever a methanol molecule and $P^1$ are in close proximity. If the reaction rate constant is similar or larger than the diffusion rate constant, the dynamics of the reaction is nonexponential.[45] We have used the model successfully in several similar studies.[29,30,46] Within the framework of the diffusive model, the well-known method of solving the model is along the lines of the Smoluchowski equation.[47]

The survival probability of $P^1$ surrounded by an equilibrium distribution of methanol, denoted by *S*, with initial condition $\rho(0) = 1$, is

$$\rho(t) = \exp(-c\int_0^t k(\tau)\, d\tau) \tag{8}$$

where $c$ is the concentration of the methanol and $k(t)$ is the time dependent rate constant, given by[48]

$$k(t) = \frac{4\pi D a_0 k_0}{k_0 + 4\pi D a_0}\left[1 + \frac{k_0}{4\pi D a_0} e^{\gamma^2 D t}\,\mathrm{erfc}((\gamma^2 D t)^{1/2})\right] \tag{9}$$

where $a_0$ is the contact radius, $\gamma$ is given by

$$\gamma = a_0^{-1}\left(1 + \frac{k_0}{4\pi D a_0}\right) \tag{10}$$

and erfc is the complementary error function. $k_0$ is the rate constant of the reaction at contact. The long-time asymptotic expression of $k(t)$ is independent of time and is given by

$$k = \frac{4\pi D a_0 k_0}{k_0 + 4\pi D a_0} \tag{11}$$

When $k_0 \ll 4\pi D a_0$, $k \approx k_0$, and $k_0$ is the rate-limiting step that determines the overall rate and not the diffusion of the reactants. When $k_0 \gg 4\pi D a_0$, the rate at long times is determined by the diffusion rate constant $k_D = 4\pi D a_0$.

*Time-Resolved Fluorescence.* Time-resolved fluorescence was detected using a time-correlated single-photon-counting (TCSPC) technique. The overall instrumental response was about 40 ps (fwhm). Measurements were taken at 10 ns full scale. The samples were excited at 310 nm. The time-resolved luminescence of C153 and C102 in hexane−methanol mixtures was measured at 10 nm intervals across the emission spectra.

Time-resolved fluorescence of coumarin in the hexane−methanol mixture was analyzed by a two-solvate reacting model, described in Scheme 1. One cannot exclusively excite one species since the shift between the bands is rather small compared with the width of each band. Therefore, the time-resolved fluorescence signal at a given time, $t$, and frequency, $\nu$, depends on the excitation frequency $\nu'$.

We calculated the signal $I_f(\nu',\nu,t)$ according to the following equation:

$$I_f(\nu',\nu,t) \propto [(1 - a(\nu'))h_1 f^1(\nu)\rho(t) + a(\nu')h_2 g^1(\nu) + (1 - a(\nu'))h_2(1 - \rho(t))g^1(\nu)]e^{-k_f t} \tag{12}$$

Here $a(\nu')$is the fraction of $P^1S^H$ generated by direct excitation of $P^0S^H$, $f^1$ and $g^1$ are the line shape functions of $P^1$ and $P^1S^H$ luminescence bands, respectively, $\rho(t)$ is the survival probability of $P^1$, and $k_f^{-1}$is the excited-state lifetime. The time dependence of $\rho(t)$, due to the hydrogen-bonding reaction, was calculated using eqs 8−10. The first term on the right-hand side of eq 12 is the luminescence intensity at frequency $\nu$ of $P^1$ excited at a frequency $\nu'$. The second term is the luminescence of $P^1S^H$ due to direct excitation at a frequency $\nu'$. The third term is the luminescence intensity growth of the $P^1S^H$ solvate due to the diffusive reaction taking place in the excited state. $h_1$ and $h_2$ are the relative fluorescence intensities of the non hydrogen bonded $P^1$ and the hydrogen bonded $P^1S^H$ species, respectively. The use of different intensities for these bands can be justified from the quantum yield and lifetime measurements of Jarzeba and co-workers.[24] They found that the quantum yield of coumarin in neat toluene, methanol and acetonitrile is $\varphi = 0.82$, 0.46, and 0.69 respectively, and the excited-state lifetimes are 5.2, 4.2, and 6.5 ns, respectively. The decrease of the quantum yield of C153 in methanol is larger than the decrease in the lifetime, which indicates a decrease in the luminescence intensity of C153 in methanol with respect to toluene. The relative luminescence intensity of the $P^1$ and $P^1S^H$ bands can be estimated from the ratio $\varphi_M\tau_M/\varphi_H\tau_H$, where M and H denote methanol and hexane, respectively. To account for the dielectric enrichment contribution to the emission band red shift (which is of the order of 400 $cm^{-1}$ for C102 at 0.83 M methanol), we shift the emission bands $g^1(\nu)$ and $f^1(\nu)$ position in a given time. The band's position is shifted exponentially with a concentration-dependent time constant. For C102 in a 0.83 M methanol mixture, the time constant is about 200 ps, similar to the value we found for the hydrogen bond exchange reaction time constant.

The parameters affecting the hydrogen-bonding dynamics are [S], $a_0$, $k_0$ and $D$. [S] is the methanol concentration, $a_0$ the contact radius for the reaction, and $k_0$ the intrinsic reaction rate constant at the contact radius. We used a value of $D \approx 3 \times 10^{-5}$ $cm^2$ $s^{-1}$ for the diffusion constant for methanol in the hexane−methanol mixture. This value is taken from Rempel and co-workers.[16] We estimated the value of $a_0$ on the basis of the size of the bare coumarin dye (3.8 Å) and our model assumption that the rate-limiting step in the hydrogen-bonding reaction is the exchange of the hexane molecule by a methanol which occurs at the interface between the first and second solvation shell. We chose a value of 4.8 Å for the reaction sphere radius as a plausible value of $a_0$. We found no significant differences for the fit to the experimental data when we used $a_0$ in the range of $4.8 < a_0 < 6.8$ Å since $k_D \geq k_0$. The relevant parameters of the fit of the hydrogen-bond dynamics are given in Table 3a. Figure 9a depicts the time-resolved luminescence at selected wavelengths for C102 in a hexane−methanol mixture of 0.65 M methanol along with the model calculated fit. At long wavelengths, >450 nm, a time growth of the fluorescence intensity was seen due to the hydrogen-bonding reaction. At these wavelengths, the $P^1S^H$ luminescence cross section was larger than that of $P^1$ since the band maximum of $P^1S^H$ was located at ~450 nm, while that of $P^1$ was at ~420 nm. Figure 9b shows the experimental time-resolved luminescence and the computer fit of C153 in a solution containing 0.83 M methanol. There was good agreement between the calculated (solid line) and experimental (open circle) fluorescence signal for both dyes, at all methanol concentrations. Because of the large bandwidth and small shift between $P^0$ and $P^0S^H$, both solvates are excited by the laser pulse at 310 nm to form $P^1$ and $P^1S^H$, respectively.

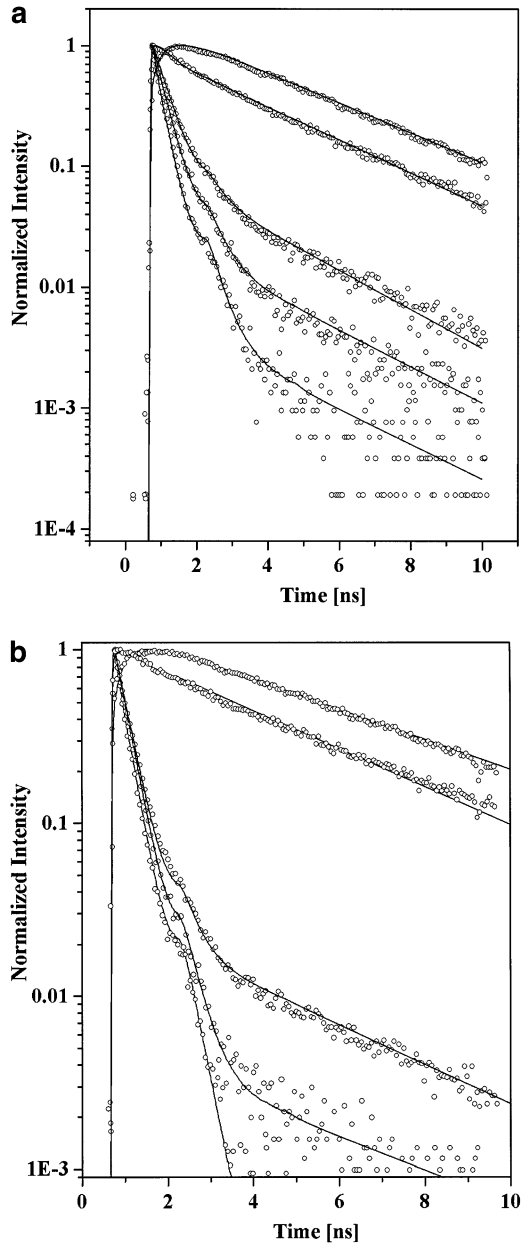


**Figure 9.** (a) Time-resolved luminescence of C102 in 0.65 M hexane−methanol mixtures at selected wavelengths: experimental curves (open circle) and computer modeling fit (solid lines). Top to bottom: 480, 440, 410, 400, and 390 nm. (b) Time-resolved luminescence of C153 in 0.83 M hexane−methanol mixtures at selected wavelengths: experimental curves (open circle) and computer modeling fit (solid lines). Top to bottom: 560, 540, 450, 440, and 430 nm.

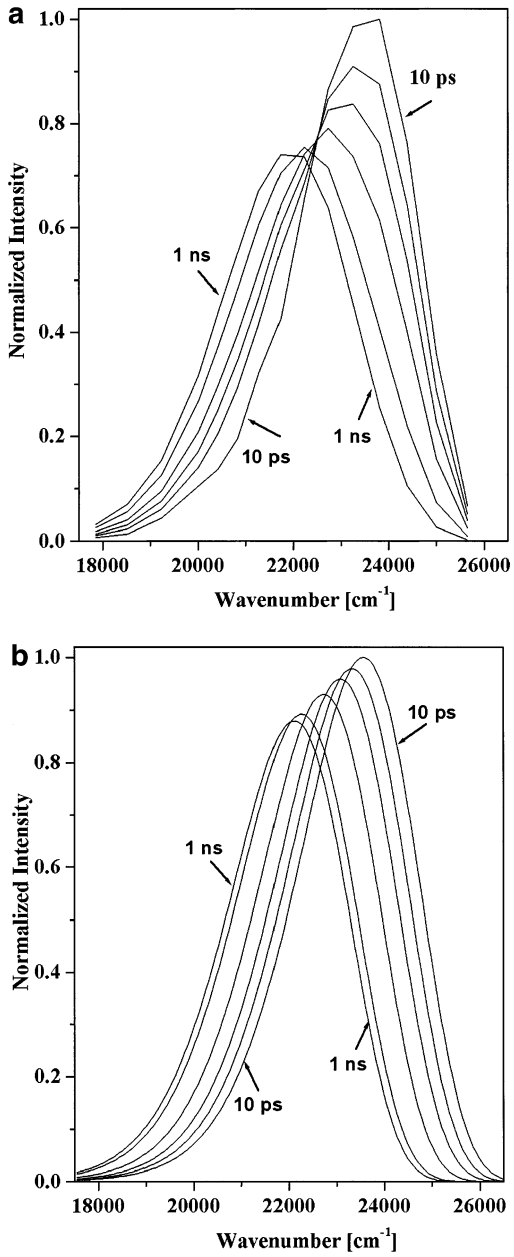


**Figure 10.** Time-resolved spectra at selected times. (a) Spectra constructed from the time-resolved emission of C102 in 0.65 M hexane−methanol mixtures. (b) Computed time-resolved spectra using the single band solvation model, (see text). The times shown from right to left: 10, 50, 100, 200, 500, and 1000 ps.

The luminescence signals at wavelengths >520 nm for the 0.83 and 0.1 M methanol concentrations differed in their relative amplitude of the component related to direct excitation. This component appears instantaneously after excitation, while the fluorescence component, due to the hydrogen bonding, has a finite rise time that depends on the methanol concentration. The relative fraction of direct excitation $P^0S^H \rightarrow P^1S^H$ for a laser excitation at 310 nm, $a(\nu')$, is given in Table 3b.

*Time-Resolved Spectra.* The experimental time-resolved spectra were constructed by a procedure given by Maroncelli and co-workers.[1] Only the long time components (>20 ps) were accurately time-resolved in this study. The time-resolved emission data collected at 10 nm intervals were fitted to a sum of exponentials using a convoluted procedure with the system IRF. Figure 10a shows the time-resolved emission spectra of C102 in a hexane−methanol mixture of 0.65 M methanol. The spectra were constructed from the time-resolved emission according to the procedure described above. Figure 10b shows the computed time-resolved spectra using the solvation model of a single band time-shifted to lower frequencies. The band's peak position and shape were determined by the best fit to the experimental band at the earliest time $t = 10$ ps, ($\upsilon_P = 23\,500$ cm$^{-1}$ $\Delta = 3000$ cm$^{-1}$, and asymmetry $\gamma = -0.24$). The total red band shift with time is 1550 cm$^{-1}$ and the exponential time constant is ~250 ps. The relative intensity of the computed bands decreases as the band shifts to the red over time due to the emission intensity dependence on the frequency.[1] As seen in Figure 10, the fit of the solvation single band red shift model is unsatisfactory. A much better fit to the time-resolved spectra is obtained using the two-solvate model, previously described in detail. We computed the time-resolved spectra for the two

**TABLE 3: Relevant Parameters of the Simulation to the Time Resolved Fluorescence of C102 and C153 in Methanol−Hexane Mixtures**

a. Simulation of the Time-Resolved Fluorescence

| probes | $D \times 10^{-5}$ ($cm^2\ s^{-1}$)[a] | $k_D \times 10^{10}$ ($M^{-1}\ s^{-1}$) | $k_0 \times 10^{10}$ ($M^{-1}\ s^{-1}$)[b] | $k \times 10^9$ ($M^{-1}\ s^{-1}$) |
|---|---|---|---|---|
| C102 | 3.0 | 1.1 | 0.4 | 2.9 |
| C153 | 3.0 | 1.1 | 0.4 | 2.9 |

b. Model Calculations to Fit the Time-Resolved Fluorescence Data

| C102 | | | | | | C153 | | | | | |
|---|---|---|---|---|---|---|---|---|---|---|---|
| $C$ (M) | $a(\nu')$ | $\Delta$ ($cm^{-1}$)[c] | $\tau_{shift}$ (ps)[d] | $V_P(P^1) \times 10^3$ ($cm^{-1}$)[e] | $V_P(P^1S^H) \times 10^3$ ($cm^{-1}$)[f] | $C$ (M) | a($\nu'$) | $\Delta$ ($cm^{-1}$)[c] | $\tau_{shift}$ (ps)[d] | $V_P(P^1) \times 10^3$ ($cm^{-1}$)[e] | $V_P(P^1S^H) \times 10^3$ ($cm^{-1}$)[f] |
| 0.4 | 0.1 | 250 | 400 | 23.8 | 22.3 | 0.1 | 0.05 | | | 22.1 | 20.9 |
| 0.65 | 0.18 | 300 | 350 | 23.7 | 22.2 | 0.83 | 0.18 | 300 | 300 | 21.0 | 19.9 |
| 0.83 | 0.2 | 400 | 200 | 23.7 | 22.2 | | | | | | |

[a] Diffusion coefficients, $D$ taken from ref 12. [b] The value of the intrinsic rate constant, $k_0$ is determined from the best fit to the time-resolved experimental data. The overall rate constants, $k$, were calculated according to eq 11. [c] The bathochromic band shift, $\Delta$ , for the contribution of the dielectric enrichment. [d] The time constant, $\tau_{shift}$, for the contribution of the dielectric enrichment. [e] The fluorescence band position at $t = 0$ of the non-hydrogen-bonded $P^1$ species. $a(\nu')$ is the relative fraction of direct excitation $P^0S^H \rightarrow P^1S^H$ for a laser wavelength at 310 nm. [f] The fluorescence band position at $t = 0$ of the hydrogen-bonded $P^1S^H$ species. $a(\nu')$ is the relative fraction of direct excitation $P^0S^H \rightarrow P^1S^H$ for a laser wavelength at 310 nm.

solvates model using eq 12 for relative contributions of the various species involved in the spectral changes. Equations 8−10 were used for the accurate dynamical changes due to the hydrogen-bonding process. Figure 11a shows the experimental time-resolved spectra at selected times; (symbols) and the computed spectra (solid lines) of C102 in a mixture containing 0.4 M of methanol. Figure 11b shows the time-resolved spectra for C153 in a solution containing 0.83 M methanol. In our model, $P^1$ converts to $P^1S^H$. As time progresses, the emission of species $P^1$ diminishes while the emission intensity of $P^1S^H$ increases. In the fitting procedure of the time-resolved spectra, the relative intensity of the hydrogen bond solvate, $h_2$ (the red band), was about 30% smaller than the blue band intensity, $h_1$.

The change in solvation energy, due to excitation of coumarin dyes in hexane−methanol mixtures, arises from three main contributions. The first is the orientational motion of the solvent molecules. The position of the maximum of the emission band of the $P^1$ species depends on the methanol mole fraction. For both coumarin dyes, at about 0.1 mole fraction of methanol, it is 1000 $cm^{-1}$ red shifted with respect to the position of the emission band of coumarin in hexane. We attribute this shift to the orientational solvation energy of the methanol molecules. The dynamics of this component are faster than the time resolution of the TCSPC technique we used in the experiment. According to Maroncelli and co-workers,[1] about 50% of the solvation energy of coumarin is gained in less than 250 fs and the longest component of the solvation dynamics is 15 ps with an amplitude of ∼0.25. The orientation solvation component shifts both $P^1$ and $P^1S^H$ bands and, at 0.1 mole fraction of methanol, it contributes ∼40% of the total band shift.

The second contribution to the solvation energy is the hydrogen bond formation in the excited state, ($P^1S^H$) which accounts for ∼50% of the total emission band shift, 1500 and 1200 $cm^{-1}$, for C102 and C153, respectively. The $P^1$ and $P^1S^H$ band position for both coumarin dyes at various methanol concentrations are given in Table 3b.

The third contribution to the solvation energy arises from the dielectric enrichment process. For C102, at relatively high methanol concentrations (>0.2 M up to 1 M), we found that both the blue and red bands shift to the red as a function of methanol concentration. The red shift of the absorption for 0.83 M methanol is 400 $cm^{-1}$. We attribute this red shift to a nonspecific contribution, which arises from nonspecific dielectric enrichment. The polar solvent (methanol) concentration next to the probe molecule is larger than that in the bulk. The red shift, due to the dielectric enrichment (400 $cm^{-1}$), is smaller than the red shift due to the hydrogen bond formation (∼1500 $cm^{-1}$). The preferential solvation process in the excited state is measured by time-resolved fluorescence. This process is relatively slow and the rate depends on the methanol concentration. For 0.83 M methanol, the rate is about $(200\ ps)^{-1}$.

## Summary and Conclusions

The work we hereby report is comprised of steady-state UV−vis absorption, emission and IR spectra, as well as time-resolved fluorescence measurements of C102 and C153 in hexane−methanol mixtures. In previous studies of electrolyte solvation of probe molecules in organic solvents, we adopted a model where a specific interaction of an ion with a probe molecule is responsible for a large portion of the solvation energy.[29,30] In this study of the solvation of coumarin dyes in a hexane−methanol mixture, we used the same concept of specific interaction of one methanol molecule at a specific site of the coumarin dyes to explain the main portion of both the absorption and emission band shifts as a function of methanol concentration. The carbonyl group of the coumarin dye is a mild base in the ground state and a stronger base in the excited state. Methanol has relatively strong acidity (in Kamlet−Taft scale $\alpha = 0.93$). IR spectra of both coumarin dyes in hexane−methanol mixtures show that the carbonyl band is blue shifted when a hydrogen bond is formed. We used a model of two distinct solvate configurations to explain the experimental data. The first species was a coumarin molecule that was not hydrogen bonded to a methanol molecule at the carbonyl group, and in the second species, a methanol molecule forms a hydrogen bond. We analyzed the absorption, steady state emission, and time-resolved emission of coumarin in a hexane−methanol mixture in a way directly related to the existence of these two distinct solvates, both in the ground and excited states. An important feature in our model is the diffusive nature of the hydrogen-bonding reaction. We demonstrated how steady state and time-resolved spectroscopic methods provide unique information for a specific hydrogen-bonding reaction. Steady-state spectroscopic techniques provide the energetics and equilibrium constants of hydrogen bonding while time-resolved spectroscopic techniques provide accurate dynamics. For C102, in a hexane−methanol mixture at high methanol concentrations above 0.1 M, we find

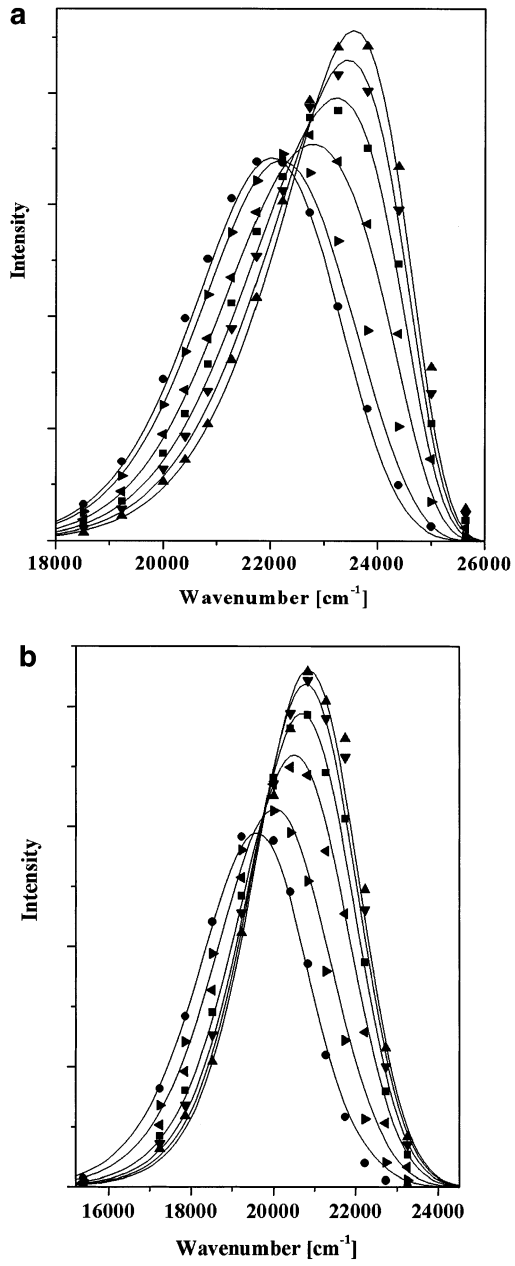


**Figure 11.** (a) Time-resolved emission spectra of C102 in 0.65 M hexane−methanol mixtures at various times: 20 (▲), 50 (▼), 100 (■), 200 (solid left triangle); 500 (solid right triangle), and 1000 (●) ps. Solid lines are computer fit. (b) Time-resolved emission spectra of C153 in 0.83 M hexane−methanol mixtures at various times: 20 (▲), 50 (▼), 100 (■), 200 (solid left triangle); 500 (solid right triangle), and 1000 (●) ps. Solid lines are computer fit.

an additional red-shift component contributing to both solvates' absorption spectra. The steady-state emission spectra of both dyes as well as the time-resolved emissions show that an addition red-shift component needs to be added to the two-solvate model. To account for this component, we invoke a nonspecific preferential solvation contribution to the red shift by the methanol molecules.

**Acknowledgment.** We thank Prof. N. Agmon for helpful discussions. This work was supported by a grant from the James-Franck German−Israel program in laser−matter interaction.

## References and Notes

(1) Horng, M. L.; Gardecki, J.; Papazyan, A.; Maroncelli, M. *J. Phys. Chem.* **1995**, *99*, 17311.

(2) Barbara, P. F.; Jarzeba, W. *Adv. Photochem.* **1990**, *1*, 15.

(3) Simon, J. D. *Acc. Chem. Res.* **1988**, *21*, 21.

(4) Bagchi, B.; Chandra, A. *Adv. Chem. Phys.* **1991**, *1*, 80. Bagchi, B. *Annu. Rev. Phys. Chem.* **1989**, *115*, 40.

(5) Ladanyi, B.; Skaf, M. S. *Annu. Rev. Phys. Chem.* **1993**, *335*, 44.

(6) Rosental, S. J.; Xie, X.; Du, M.; Fleming, G. R. *J. Chem. Phys.* **1991**, *95*, 4715.

(7) Suppan, P. J. *Chem. Soc., Faraday Trans. 1* **1987**, *83*, 495.

(8) Khajehpour, M.; Kauffman, J. F. *J. Phys. Chem. A* **2000**, *104*, 7151.

(9) Khajehpour, M.; Welch, C. M.; Kleiner, K. A.; Kauffman, J. F. *J. Phys. Chem. A* **2001**, *105*, 5372.

(10) Petrov, N. K.; Wiessner, A.; Fiebig, T.; Straerk, H. *Chem. Phys. Lett.* **1995**, *241*, 127.

(11) Petrov, N. K.; Wiessner, A.; Straerk, H. *J. Chem. Phys.* **1998**, *108*, 2326.

(12) Cichos, F.; Willert, A.; Rempel, U.; von Borczyskowski, C. *J. Phys. Chem. A* **1997**, *101*, 8179.

(13) Schatz, T. R.; Kobetic, R.; Piotrowiak, P. *J. Photochem. Photobiol. A* **1997**, *105*, 249.

(14) Nishiyama, K.; Okada, T. *J. Phys. Chem. A* **1998**, *102*, 9729.

(15) Ferreira, J. A. B.; Coutinho, P. J. G.; Costa, S. M. B.; Martinho, J. M. G. *Chem. Phys.* **2000**, *262*, 453.

(16) Cichos, F.; Brown, R.; Rempel, U.; von Borczyskowski, C. *J. Phys. Chem. A* **1997**, *101*, 8179.

(17) Day, T. J. F.; Patey, G. N. *J. Chem. Phys.* **1999**, *111*, 10937.

(18) Raju, B. B.; Costa, S. M. B. *Phys. Chem. Chem. Phys.* **1999**, *1*, 3539.

(19) Andrade, S. M.; Costa, S. M. B. *Phys. Chem. Chem. Phys.* **1999**, *1*, 4213.

(20) Jarzeba, W.; Walker, G. W.; Johnson, A. E.; Barbara, P. F. *Chem. Phys.* **1991**, *152*, 57.

(21) Gardecki, J.; Maroncelli, M. *Chem. Phys. Lett.* **1999**, *301*, 571.

(22) Molotsky, T.; Huppert, D. *J. Phys. Chem. A* **2002**, *106*, 8525.

(23) Agmon, N. *J. Phys. Chem. A* **2002**, *106*, 7256.

(24) Frolicki, R.; Jarzeba, W.; Mostafavi, M.; Lampre, I. *J. Phys. Chem. A* **2002**, *106*, 1708.

(25) Solntsev, K. M.; Huppert, D.; Tolbert, L. M.; Agmon, N. *J. Am. Chem. Soc.* **1998**, *120*, 7981.

(26) Solntsev, K. M.; Huppert, D.; Agmon, N. *J. Phys. Chem. A* **1999**, *103*, 6984.

(27) Fainberg, B. D.; Narbaev, V. *J. Chem. Phys.* **2000**, *113*, 8113.

(28) See: Fraser, R. D. B.; Suzuki, E. In *Spectral Analysis*; Blackburn. J. A., Ed.; Marcel Dekker: New York, 1970: p 171.

(29) Argaman, R.; Molotsky, T.; Huppert, D. *J. Phys. Chem. A* **2000**, *104*, 7934.

(30) Argaman, R.; Huppert, D. *J. Phys. Chem. B* **2000**, *104*, 1338.

(31) Kamlet, M. J.; Abboud, J. L. M.; Abraham, M. H.; Taft, R. W. *J. Org. Che*m. **1983**, *48*, 2887.

(32) Laurence, Ch.; Nicolet, P.; Dalati, M. T.; Abboud, J.-L. M.; Notario, R. *J. Phys. Chem.* **1994**, *98*, 5807.

(33) Chapman, C. F.; Maroncelli, M. *J. Phys. Chem.* **1991**, *95*, 9095.

(34) Gustavsson, T.; Cassara, L.; Gulbinas, V.; Gurzadyan, G.; Mialocq, J.-C.; Pommeret, S.; Sorgius, M.; van der Meulen, P. *J. Phys. Chem. A* **1998**, *102*, 4229.

(35) Moog, R. S.; Bankert, D. L.; Maroncelli, M. *J. Phys. Chem.* **1993**, *97*, 1496.

(36) Nibbering, E. T. J.; Tschirchwitz, F.; Chudoba, C.; Elsaesser, T. *J. Phys. Chem. A* **2000**, *104*, 4236.

(37) Ladanyi, B. M.; Skaf, M. S. *J. Phys. Chem.* **1996**, *100*, 18258.

(38) Sarkar, N.; Das, K.; Datta, A.; Das, S.; Bhattacharyya, K. *J. Phys. Chem.* **1996**, *100*, 100523.

(39) Mandal, D.; Datta, A.; Pal, S. K.; Bhattacharyya, K. *J. Phys. Chem. B* **1998**, *102*, 9070.

(40) Raju, B. B.; Costa, S. M. B. *Phys. Chem. Chem. Phys.* **1999**, *1*, 5029.

(41) Oster, G. *J. Am. Chem. Soc.* **1946**, *68*, 2036.

(42) Kirkwood, J. G. *J. Chem. Phys.* **1939**, *7*, 911.

(43) Böttcher, C. J. F.; Bordewijk, P. *Theory of Electric Polarization*; Elsevier: Amsterdam, 1973; Vol. 1.

(44) Ireland, J. F.; Wyatt, P. A. H. *Adv. Phys. Org. Chem.* **1976**, *12*, 131.

(45) Szabo, A. *J. Phys. Chem.* **1989**, *93*, 6929.

(46) Cohen, B.; Huppert, D.; Agmon, N. *J. Phys. Chem. A* **2001**, *105*, 7165.

(47) von Smoluchowski, M. *Z. Phys. Che*m. **1917**, *92*, 129.

(48) Collins, F. C.; Kimball, G. E. *J. Colloid Sci.* **1949**, *4*, 425.